View metadata, citation and similar papers at core.ac.uk

brought to you by CORE

provided by Repositorio INDICASAT AIP

Provided for non-commercial research and education use.
Not for reproduction, distribution or commercial use.

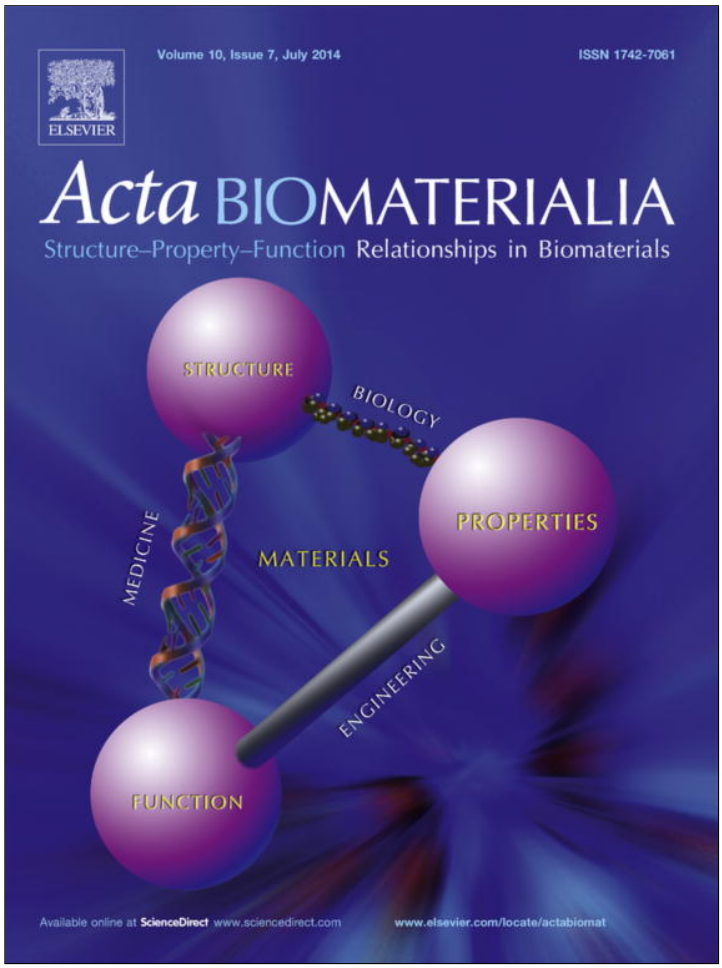

This article appeared in a journal published by Elsevier. The attached copy is furnished to the author for internal non-commercial research and education use, including for instruction at the authors institution and sharing with colleagues.

Other uses, including reproduction and distribution, or selling or licensing copies, or posting to personal, institutional or third party websites are prohibited.

In most cases authors are permitted to post their version of the article (e.g. in Word or Tex form) to their personal website or institutional repository. Authors requiring further information regarding Elsevier's archiving and manuscript policies are encouraged to visit:

http://www.elsevier.com/authorsrights

Author's personal copy

Acta Biomaterialia 10 (2014) 2894–2906

Contents lists available at ScienceDirect

Acta Biomaterialia

journal homepage: www.elsevier.com/locate/actabiomat

Review

A review on the wettability of dental implant surfaces I: Theoretical and experimental aspects

Frank Rupp [a,*,1], Rolando A. Gittens [b,1], Lutz Scheideler [a], Abraham Marmur [c], Barbara D. Boyan [d], Zvi Schwartz [d,e], Jürgen Geis-Gerstorfer [a]

[a] Department of Prosthetic Dentistry, Section Medical Materials and Technology, University Hospital Tübingen, Tübingen, Germany
[b] Center for Biodiversity & Drug Discovery, Institute for Scientific Research and High Technology Services (INDICASAT-AIP), Panama, Panama
[c] Chemical Engineering Department, Technion – Israel Institute of Technology, Haifa, Israel
[d] Department of Biomedical Engineering, Virginia Commonwealth University, Richmond, VA, USA
[e] Department of Periodontics, University of Texas Health Science Center at San Antonio, San Antonio, TX, USA

ARTICLE INFO

Article history:
Available online 28 February 2014

Keywords:
Wettability
Hydrophilicity
Surface energy
Contact angle hysteresis
Roughness induced wetting

ABSTRACT

The surface wettability of biomaterials determines the biological cascade of events at the biomaterial/host interface. Wettability is modulated by surface characteristics, such as surface chemistry and surface topography. However, the design of current implant surfaces focuses mainly on specific micro- and nanotopographical features, and is still far from predicting the concomitant wetting behavior. There is an increasing interest in understanding the wetting mechanisms of implant surfaces and the role of wettability in the biological response at the implant/bone or implant/soft tissue interface. Fundamental knowledge related to the influence of surface roughness (i.e. a quantification of surface topography) on titanium and titanium alloy surface wettability, and the different associated wetting regimes, can improve our understanding of the role of wettability of rough implant surfaces on the biological outcome. Such an approach has been applied to biomaterial surfaces only in a limited way. Focusing on titanium dental and orthopaedic implants, the present study reviews the current knowledge on the wettability of biomaterial surfaces, encompassing basic and applied aspects that include measurement techniques, thermodynamic aspects of wetting and models predicting topographical and roughness effects on the wetting behavior.

© 2014 Acta Materialia Inc. Published by Elsevier Ltd. All rights reserved.

1. Introduction

The surface wettability of a biomaterial in combination with other surface characteristics, such as the micro- and nanotopography, surface energy, charge and functional groups, determine with unknown influential weight the biological cascade of events at the biomaterial/host interface that encompasses from protein adsorption to hard- and soft-tissue interactions to bacterial film formation [1–10]. Decades of interdisciplinary research in the field of dental biomaterials led to the clinical success of titanium implants for bone applications. After recognizing that titanium can establish an intimate and direct interaction with bone, termed osseointegration, the metal and its alloys have been used for more than 40 years in the partly or full edentulous mandible and maxilla, as root replacement for the anchorage of prostheses, crowns or bridges [11–13].

Albrektsson et al. pioneered the concept of a possible role for surface finish on the biological response to an implant [14]. Since then, tremendous efforts have been made to gain deeper insight into the role of surface topography for bone formation. A prerequisite has been to properly describe surface topography by measuring the length-scale dependent surface roughness. After separating short-wave roughness from long-wave waviness (e.g. Gaussian filtering), a set of roughness parameters is acquired for the parameterization and quantification of topography [15]. These parameters, extracted from two-dimensional (2-D) surface profiles or three-dimensional (3-D) surface topographies, can be assigned to different groups such as surface height, spatial, hybrid or functional parameters. Guidelines developed for the characterization of implant surfaces suggest that topographical descriptions should include a set of roughness parameters from each of these groups [16].

* Corresponding author. Address: Department of Prosthetic Dentistry, Section Medical Materials & Technology, University Hospital Tübingen, Osianderstr. 2-8, D-72076 Tübingen, Germany. Tel.: +49 7071 29 80967.
E-mail address: frank.rupp@med.uni-tuebingen.de (F. Rupp).
[1] These authors contributed equally to this work.

http://dx.doi.org/10.1016/j.actbio.2014.02.040
1742-7061/© 2014 Acta Materialia Inc. Published by Elsevier Ltd. All rights reserved.

Author's personal copy

Until today, however, clinical studies have often lacked any investigation of implant surface roughness or give only limited information of the topographies by presenting only the 2-D mean average roughness, R_a, or the 3-D analog, S_a. A recent systematic review of in vivo data on bone response to titanium surface topography concluded that moderately rough surfaces with S_a between 1 and 2 μm seem to better optimize osseointegration at the dental implant/bone interface than smoother (< 1 μm) or rougher (> 2 μm) surfaces [17]. However, average roughness values above 2.5 μm have also been shown to be very successful clinically [18–21]. Roughness analyses of clinical dental implants (i.e. cylindrical shaped) are yet not standardized, and absolute values of single roughness parameters have to be compared and interpreted with caution. Very recently, the focus has shifted from evaluating solely microtopographical surface features to include the analysis of the role of nanotopographical surface irregularities in the cascade of events at the implant/bone interface [22–24].

Based on biomaterials studies in the 1980s [25–27], later studies focused in more detail on the role of material surface properties in the wound healing response and formation of new bone around the implant [28–30]: surface chemistry and specific surface energy (i.e. surface free energy, surface tension), in addition to surface topography, were revealed to be critical factors that could affect cellular response. Some studies have also evaluated the role of conditioning films (e.g. the surface-dependent formation of the acquired macromolecular salivary pellicle), which influence bacterial plaque accumulation associated with implant failure (i.e. peri-implantitis) [31].

Compared to the large number of studies highlighting the role of surface topography on the biological response, relatively few studies have been reported within the last two decades on the wettability or surface energy of dental and orthopedic implants. Recently, however, an increasing number of studies have addressed the wetting behavior of dental implants. Our group reported an *in vitro* study on the hydrophilicity of marketed dental implants from several manufacturers [32]. In addition, the role of wettability on titanium implants was recently evaluated both *in vitro* [3,33] and *in vivo* [34,35]. Still, correlations between surface wettability and corrosion, which have been thoroughly evaluated in materials' oriented disciplines such as atmospheric corrosion [36], are only beginning to be determined in the dental implant field.

Our aim is to contribute to the scarce information on the literature on theoretical and experimental aspects of wettability in the field of biomaterial and implant surfaces. This review addresses physicochemical aspects of implant wettability with a special focus on the wetting behavior of titanium implants. First, we review the basic aspects concerning different approaches for the measurement of wettability of experimental samples and of clinical implants by contact angle (CA) analysis. Second, a description follows of the fundamental role of specific surface energy for the wetting behavior. Finally, different aspects concerning the influence of roughness on the wetting behavior are highlighted. To avoid misinterpretations, the terminology used in this review concerning the different types of theoretically derived and experimentally accessible contact angles (CAs) follows the definitions of Marmur [37].

2. Experimental approaches to the analysis of wettability

Several common approaches for the analysis of surface wettability have been adapted to titanium implant surfaces. The most common approach to gain insight into the wetting behavior of a given solid material is called the sessile drop technique, in which a drop of a desired wetting liquid is placed on the surface of the specimen, and the angle between the tangent of the drop at the solid/liquid/gas three-phase boundary and the horizontal baseline of the solid surface is measured (Fig. 1a). This angle, the so-called contact angle (CA or θ), quantifies the wetting of the surface by the specific liquid used.

For example, the CA characterizes the hydrophilicity of the surface if water has been used as the wetting agent. In principle, the CA can range from 0 to 180°, indicating that the wetting liquid is being drawn towards the surface (i.e. spreading of the drop) or is being repelled by the surface (i.e. beading of the drop), respectively. Water CAs lower than 90° designate surfaces as hydrophilic, while CAs very close to 0° ascribe surfaces a superhydrophilic characteristic. Surfaces with water CAs above 90° are considered hydrophobic, and surfaces with CAs above 150°, where the wetting is strongly hindered, are often termed superhydrophobic surfaces.

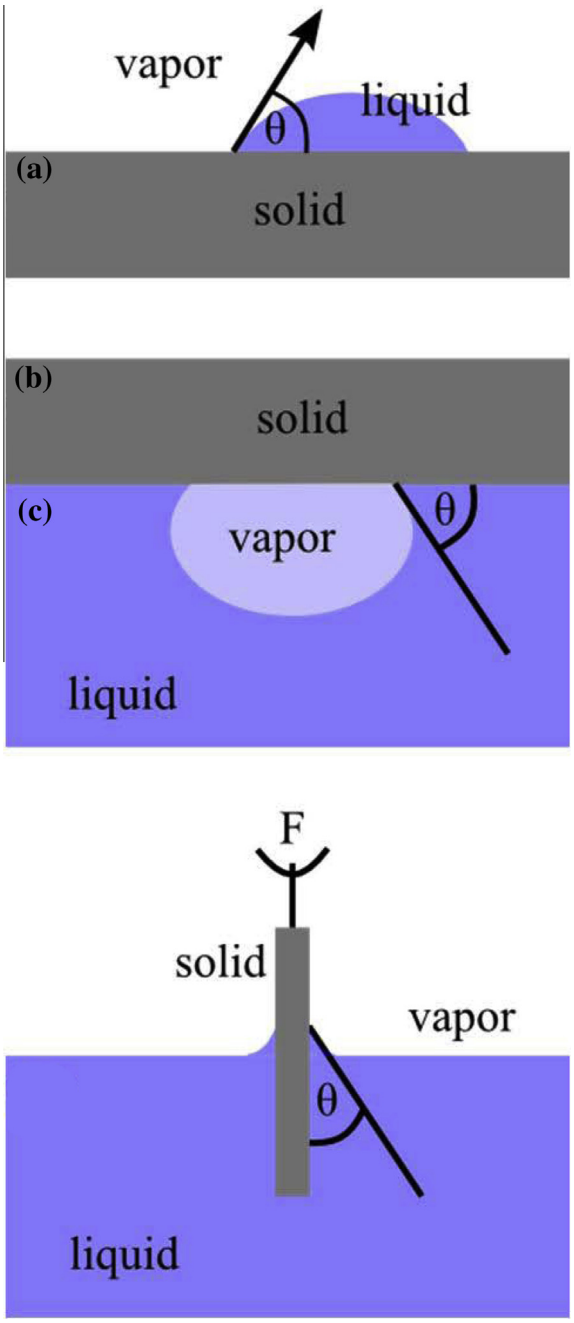

Fig. 1. Contact angle as measured by different techniques: (a) sessile drop technique, (b) captive bubble technique and (c) the Wilhelmy balance technique.

Author's personal copy

Surface characteristics can influence the measured CAs, and the basic principles of how surface roughness, specifically, can affect wetting are highlighted in Section 3. It has to be noted that the terminology of wetting is not well defined and suggestions for a more precise classification methodology and terminology have been recently published [38].

In the case of the sessile drop technique, two main types of forces produce the shape of the drop: surface tension forces, which tend to minimize the total surface energy of the droplet by producing a spherical shape with the proper contact angle; and the gravitational force, which tends to flatten and spread the drop over the surface. The competition between these two effects is expressed by the dimensionless Bond number (B_o), which is defined by:

$$B_o = \frac{\rho r^2 g}{\gamma_{lv}} = \left(\frac{r}{L_c}\right)^2 \quad (1)$$

where γ_{lv} is the liquid–vapor surface tension, ρ the liquid density, r a typical radius of the drop, g the gravitational acceleration and L_c is defined as the capillary length (Eq. (2)). A low Bond number (< 1) indicates that surface tension dominates, whereas a high Bond number indicates stronger gravitational effects. In the case of a very strong gravitational influence caused by a large drop volume, the drop does not have a spherical shape but instead ends up with an elongated and flattened shape that is less convenient for CA measurements. For gravity to be negligible according to Eq. (1), the base radius of a sessile drop has to be smaller than the capillary length L_c of the liquid used:

$$L_c = \sqrt{\frac{\gamma_{lv}}{\rho g}} \quad (2)$$

Thus, to avoid gravitational deformations using water as the wetting liquid, the volume of the drop resting on a horizontal surface should be small enough to form a drop shape with a base radius below L_c of 2.7 mm. In practice, water droplets of 1–5 μl are commonly used. Besides water, other liquids are in use for CA measurements and surface free energy estimations, such as ethylene glycol (L_C = 2.1 mm) and diiodomethane (L_C = 1.3 mm). To avoid gravity-caused deformations, these liquids with lower L_C require droplets with correspondingly smaller volumes (usually 1–2 μl) to obtain a resting droplet with spherical shape in the course of CA analysis. When considering surface roughness, the base radius of a sessile drop should be about three orders of magnitude larger than the typical dimension (wavelength) of heterogeneity (i.e. surface roughness or chemical variation) for accurate CA measurements, leading to the general suggestion to use drops as large as possible relative to the scale of the roughness for the appropriate characterization of apparent CAs [39–42]. Therefore, the drop volume used for a specific wetting experiment should be carefully chosen considering the wetting liquid, the base radius of the sessile drop and the roughness properties of the surface under investigation. Defining the ideal drop volume for accurate CA measurements is still under intense research.

In recent years, novel experimental techniques for producing and imaging nanoscale droplets were developed, allowing wetting analysis with much better spatial resolution than with classical macroscopic approaches. Atomic force microscopy (AFM) has been combined with different techniques for the direct deposition of micro- and nanosized droplets such as atomizers or electrospraying, thus allowing high accuracy measurement of contact line curvature and contact angle [43,44]. Another interesting technique is environmental scanning electron microscopy (ESEM), which allows real-time observation of the in situ nucleation of micrometer-sized droplets in its low-vacuum video-monitored chamber [33,44–46]. Both of these techniques have increased our knowledge in this challenging field.

Problems using small drops arise on the one hand from evaporation and on the other hand from line tension limitations. Whereas CAs of macroscopic droplets are not significantly influenced by evaporation during the measurement time, such phenomena cannot be neglected if ultrasmall droplets are experimentally produced on surfaces, which limits the time available for CA measurements [44]. Furthermore, line tension may interfere and cause variations in the CA measurements of smaller nanoscopic drop sizes, making the analysis of the results possibly very complex [47–49]. Keeping in mind the above mentioned requirements for the drop size, the respective wavelength of roughness underlying the drop and influencing the CA also has to be considered, because nanoroughness influences the CA in these cases rather than microroughness. Fig. 2 summarizes critical factors that influence the shape of a sessile drop dependent on the drop volume and the surface topography.

Regarding biological events at rough implant surfaces, our focus is shifting from microscale to nanoscale features that obviously not only influence cellular interactions but also interfere with macromolecules that form conditioning films under physiological conditions (e.g. on implants facing blood or saliva) [6]. Therefore, considering the important role of nanoscale features at biomaterial surfaces, wettability studies using nanodroplets may shed new light on the underlying interfacial reactions.

Generally, the sessile drop technique, if properly done, allows the measurement of a few types of contact angles. "Static" measurements investigate the equilibrium shape of the droplet after spreading has finished (the term "static" may be misleading, since the process of spreading is dynamic). This is a less recommended methodology, since it may lead to different results in different labs [50,51]. The CA that should be reproducible and susceptible to theoretical analysis is the most stable CA [50–52], which may be reached after exposing the drop to controlled vibrations. "Dynamic" measurements are realized by moving the interface, so that the water front moves towards the vapor phase or moves away from it. The highest measured CA in the former experimental situation is the advancing CA, the latter is the receding CA (again, the term "dynamic" is somewhat misleading since the motion of the liquid front is dynamic, however the measured CAs represent (metastable) equilibrium states). A moving interface can also be investigated by increasing and decreasing the drop volume, which can be achieved by adding and removing liquid with a syringe in direct contact with the drop, while continuously monitoring the drop shape to capture the largest and lowest possible angles, respectively. The difference of advancing and receding CAs, what is called the CA hysteresis, is highlighted in detail in Section 3. Sometimes it is difficult to get reliable results for dynamic CAs by the sessile drop technique due to disturbances on the drop geometry by the syringe needle, especially in the case of very small receding angles.

An alternative method for dynamic CA measurements is the so-called Wilhelmy plate method [53–55]. This method uses force measurements for CA calculations acquired by dipping a sample

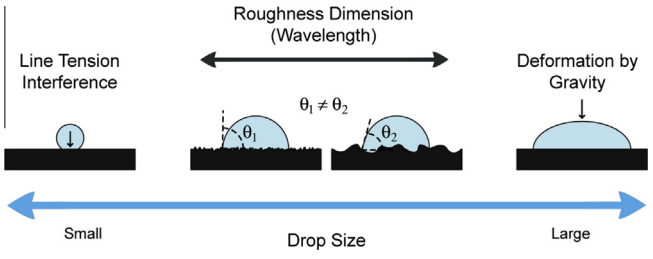

Fig. 2. Critical factors that influence the shape of a sessile drop dependent on the drop volume: line tension at nanodroplets, the drop size in relation to surface waviness and gravity induced deformations at larger drops.

Author's personal copy

of known geometry, fixed to an electrobalance, into the wetting liquid (Fig. 1c). The total force acting on a sample of rectangular shape (i.e. a plate) partially immersed in a wetting liquid is composed of the sample weight (F_G) and the Wilhelmy force (F_W) minus the buoyancy force (F_B) [56]:

$$F = F_G + F_W - F_B = mg + cos\theta L\gamma_{lv} - V\rho g \quad (3)$$

where F is the total force exerted on the liquid, m is the mass of the sample plate, g is the acceleration due to gravity, θ is the contact angle, L is the perimeter of the immersed sample (wetted length), γ_{lv} is the liquid–vapor surface tension, V is the volume of the immersed part of the sample and ρ is the density of the liquid. Eq. (3)is simplified first by a reset of the balance to zero before each run (i.e. $F_G = 0$) and second by a linear regression of the detected immersion and emersion forces to zero immersion depth (i.e. $F_B = 0$), thus eliminating both weight and buoyancy and making the CAs easily accessible via the tensiometric forces.

$$cos\theta = \frac{F_W}{L\gamma_{lv}} \quad (4)$$

One advantage of the Wilhelmy plate method is that receding CAs can be just as easily accessed as advancing CAs. This is possible by a time-resolved detection of force values during continuously immersing and emerging the sample into the liquid [57]. Another advantage is that long-term measurements are possible because wetting is not disturbed by evaporation as fast as with small sessile droplets. Some drawbacks exist that limit the application in some cases. One of them is that the reported angle is the average over the entire perimeter line of intersection of the liquid with the solid. If the front and back faces of a sample disc have been treated differently, then the average value may have little significance, and the same is true if the surface energy is not highly uniform across the area of interest [57]. However, this may also be an advantage because the method yields very accurate average values, which is not possible to access on a large area by sessile droplets. The Wilhelmy method requires a clear knowledge of the sample geometry concerning the respective perimeter at each immersion depth. Furthermore, to calculate the CAs from the Wilhelmy force loops, one has to first measure the surface tension of the liquid. However, several methods are available to experimentally access the surface tension; one of them, the Wilhelmy plate method itself, uses for this purpose a plate with a well-defined surface with a given CA of 0°. The Wilhelmy balance method has been reported to be the most accurate and least subjective technique for measuring CA hysteresis [54,58]. A simple Wilhelmy experiment consists of one single immersion and emersion run and may result in a typical force loop as depicted in Fig. 3.

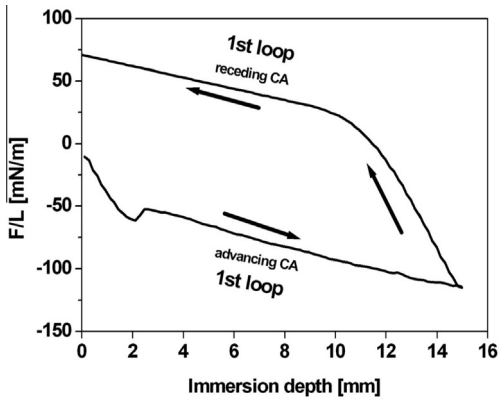

Fig. 3. Exemplary force loop of the Wilhelmy balance method showing one advancing and one receding force curve indicating thermodynamic CA hysteresis. From the respective curves, the advancing and receding contact angles are calculated.

Whereas both the sessile drop and the tensiometric Wilhelmy technique have been often applied for investigations of titanium specimens, another technique, the captive bubble technique, also allows an experimental approach to CAs [59]. This inverse technique evaluates the air/water interface by submerging a solid material in the wetting liquid and dispensing from a capillary syringe an air bubble underneath the solid (Fig. 1b).The receding CA is measured by increasing the volume of the bubble, whereas the advancing CA can be captured by retracting back the air into the syringe and reducing the volume of the bubble. This method appears to be especially suitable for hydrophobic materials [60]. Table 1 summarizes advantages and drawbacks of goniometric and tensiometric techniques.

3. Thermodynamic aspects of wetting: Young's equation and surface free energy

Before the basic aspects of how roughness influences wetting are discussed in Section 4, it is essential to describe in more detail an axisymmetric drop resting on a smooth surface. Given that the drop rests on an ideal flat and homogeneous surface in thermodynamic equilibrium, the drop shape with the characteristic ideal CA θ is solely formed as a result of the liquid/vapor (γ_{lv}), solid/liquid (γ_{sl}), and solid/vapor (γ_{sv}) interfacial tensions, according to Young's equation that was published over 200 years ago [61]:

$$\cos\theta_{Young}\gamma_{lv} = \gamma_{sv} - \gamma_{sl} \quad (5)$$

The interfacial tensions acting at the three-phase line are visualized in Fig. 4a. Generally, surface tension is caused by the asymmetry of the cohesive forces of molecules at a surface compared to

Table 1
Advantages and drawbacks of different measurement techniques for static, advancing (adv.) and receding (rec.) contact angles (CAs).

	Sessile drop	Captive bubble	Wilhelmy balance
Sample type (geometry)	Discs, plates (arbitrary form)		Rectangular plates, cylinders, fibers (geometrically defined perimeter)
Sample type (surface)	Frontside of interest may differ from the backside		Both sides have to be identical
Surface heterogeneity	Heterogeneity captured by individual measurements at different positions. Averages not accurate		Heterogeneity not detectable. Accurate average over the wetted length at each immersion depth
Accuracy of CA analysis	Dependent on algorithms for drop shape analysis and on individually positioned baselines		Dependent on the interval chosen for linear regression
CA hysteresis	Complicated, especially for small rec. CA due to the syringe sticking in the drop	By changing the air bubble volume adv. and rec. CAs can be measured	Rec. CAs as easily measured as adv. CAs. Multi-loop runs reveal kinetic hysteresis
Liquid volume	Dependent on capillary length L_c of liquid and wavelength of surface heterogeneity	Higher amounts of liquid necessary	
Dehydration of the solid	Sensitive, a dry surface is investigated	Unproblematic, the material is immersed	Sensitive, the material/air interface is moving

Author's personal copy

(a)

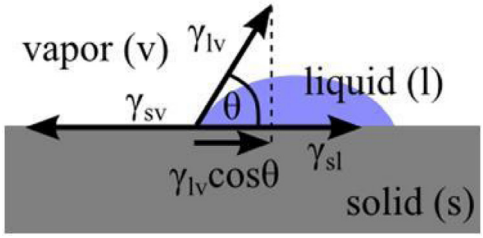

(b)

Energetic relationship	CA relationship	Optical representation	Macroscopic result
$\gamma_{sv} - \gamma_{sl} > 0$	$0° \le \theta \le 90°$		High wettability
$\gamma_{sv} - \gamma_{sl} > \gamma_{lv}$	$\theta = 0°$		Complete wetting (spreading)
$\gamma_{sv} - \gamma_{sl} < 0$	$90° \le \theta \le 180°$		Low wettability
$\gamma_{sl} - \gamma_{sv} > \gamma_{lv}$	$\theta = 180°$	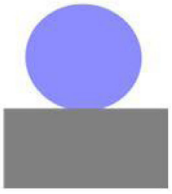	Non-wetting

Fig. 4. (a) Schematic diagram showing the static contact angle of a liquid droplet on an ideal solid surface and the graphical derivation of Young's equation. (b) Interrelations between wetting tension and the wetting of a solid. To improve wetting, the surface tension of the wetting liquid should be lower than the surface tension of the solid substrate.

molecules in the bulk where each molecule has surrounding partners resulting in a net force of zero. Correspondingly, the surface energy is minimized in the bulk, whereas at the surface the energy is increased due to the missing surrounding molecules. Therefore, to reduce surface energy, the surface area has to be minimized, thus resulting in phenomena like spherical water drops or the spreading of aqueous liquids on higher energetic surfaces. Whereas the CA and the liquid's surface tension (γ_{lv}) are experimentally accessible, this is not the case for the solid/liquid (γ_{sl}) interfacial tension or for the surface tension of the solid (γ_{sv}), often denoted the specific free energy (Gibbs energy) of the solid surface. As seen from Young's equation, only the wetting tension γ_{sv}–γ_{sl}, but not the surface tension of the solid itself is experimentally accessible. Fig. 4b shows interrelations of the wetting tension and the CA.

Wetting is favored by combining high energetic solid surfaces and wetting liquids with low surface tension. As mentioned above, during wetting, the exposed area of a high energetic surface is reduced in favor of a solid/liquid interface, thus lowering the energy of the complete system as much as possible to reach a (meta)stable equilibrium state. A plausible way to enhance wetting, which has been associated with improved implant success, is therefore to increase the surface tension of biomaterials [10,34,62]. Any wetting with a CA below 90° requires a positive wetting tension, considering the respective wetting tensions of aqueous bioliquids of interest. Water itself is a relatively high energetic polar liquid due to the formation of hydrogen bonds. The surface tension of water is ~73 mN m^{-1} at room temperature. In contrast, the surface tension of blood has been measured at 52 mN m^{-1} at 37 °C [63], and that of

Author's personal copy

saliva has been reported in the range of 53.4 to 63.2 mN m^{-1} [64,65].

Besides Young's equation, an additional equation is necessary to acquire information about the surface free energy of a solid material of interest. Several empirical or semi-empirical approaches have been proposed to estimate this important surface parameter. The geometric mean calculation of surface free energy, an approach often used in materials science, divides the total surface free energy γ_{tot} of a solid or a liquid in hydrogen bonding (polar) γ^p and non-polar γ^d components:

$$\gamma_{tot} = \gamma^p + \gamma^d \tag{6}$$

Owens and Wendt proposed that the geometric mean combined the polar and dispersion components of the solid and liquid surface interfacial energies [66]:

$$\gamma_{sl} = \gamma_{sv} + \gamma_{lv} - 2\sqrt{\gamma^d_{sv}\gamma^d_{lv}} - 2\sqrt{\gamma^p_{sv}\gamma^p_{lv}} \tag{7}$$

After combining Eq. (7)with Young's equation (Eq. (3)), the following linear equation ($y = ax + b$) can be obtained:

$$\frac{1+\cos\theta}{2}\frac{\gamma_{lv}}{\sqrt{\gamma^d_{lv}}} = \sqrt{\gamma^p_{sv}}\sqrt{\frac{\gamma^p_{lv}}{\gamma^d_{lv}}} + \sqrt{\gamma^d_{sv}} \tag{8}$$

Thus, CA measurements with several test liquids can provide estimates of the polar and dispersion components of the surface free energy, when subjected to linear regression, by calculating y-axis intercepts and slopes, respectively, and using the squared value. Kaelble proposed taking the mean of paired CAs of two test liquids with known total surface tension and polar and dispersive components to calculate the solid's energy values according to the Owens–Wendt equation [67].

The Lifshitz-van der Waals/acid–base (LW–AB) approach also divides the total surface free energy of solids or liquids in components, which in this case are the nonpolar Lifshitz-van der Waals (LW) and the polar Lewis-acid–base (AB) components [68].

$$\gamma_{tot} = \gamma^{LW} + \gamma^{AB} \tag{9}$$

The electron acceptor γ^+ (Lewis-acid) and the electron donor γ^- (Lewis-base) components are related to the total acid–base component γ^{AB} according to the following equation:

$$\gamma^{AB} = 2\sqrt{\gamma^+\gamma^-} \tag{10}$$

The manner in which the solid and liquid surface tensions are combined to yield the solid/liquid interfacial tension differs drastically between the γ^{LW} and γ^{AB} components [69], so that finally one of the two unknowns in the Young equation, γ_{sl}, can be calculated as follows:

$$\gamma_{sl} = \left(\sqrt{\gamma^{LW}_{sv}} - \sqrt{\gamma^{LW}_{lv}}\right)^2 + \left(\sqrt{\gamma^+_{sv}\gamma^-_{lv}} + \sqrt{\gamma^+_{sv}\gamma^-_{lv}}\right) - 2\left(\sqrt{\gamma^+_{sv}\gamma^-_{lv}} - \sqrt{\gamma^-_{sv}\gamma^+_{lv}}\right) \tag{11}$$

Similarly to the geometric mean approach, CA measurements with different liquids enable the determination of the electron acceptor and electron donor components of the solid. However, CA data of three liquids with known surface tension components γ^{LW}, γ^+, γ^- are needed, since after combining with Young's equation, three unknowns are in the final expression using the LW–AB approach, as shown below:

$$(1+\cos\theta)\gamma_{lv} = -2\left(\sqrt{\gamma^{LW}_{sv}\gamma^{LW}_{lv}} + \sqrt{\gamma^+_{sv}\gamma^-_{lv}} - \sqrt{\gamma^-_{sv}\gamma^+_{lv}}\right) \tag{12}$$

Bellon-Fontaine et al. [70] found serious deviations between surface free energy (SFE) values calculated by different approaches. Combe et al. [71] clearly demonstrated and discussed problems related to SFE measurements and calculations. For example, there is currently no standard procedure for which test liquids should be used, and literature data on thermodynamic properties of many liquids are contradictory. Furthermore, the choice of the set of liquids has to be done carefully to avoid errors during SFE calculations [72]. In addition, there is an ongoing discussion on methods for SFE calculations based on CA data [73]. Above, two common approaches for SFE estimation have been reviewed. More detailed information about different mathematical methods is given by Sharma and Rao [74]. Compared to other approaches, the LW–AB method has shown the most internal consistency when applied to microbial cell surfaces [74] and therefore currently seems to be a sophisticated method for the characterization of the thermodynamics of biomaterial and biological systems [75,76]. Also other approaches, such as the Zisman approach that allows the calculation of the so-called critical surface tension, have been applied on dental implant materials [28]. Recent efforts to find a correlation between interfacial tensions and corresponding surface tensions [73] have to be evaluated closely for their possible importance in the biomaterials field.

E. A. Vogler ascribed to the adhesion tension (wetting tension) a more predictive role for biological responses than to surface energetic parameters [77]. In contrast to the above described technical dividing line between hydrophilic and hydrophobic at a water CA of 90°, corresponding to an adhesion tension of zero, Vogler defined hydrophobic surfaces already as those exhibiting water CA > 65° corresponding to an adhesion tension < 30 mN cm^{-1}. Indeed, it seems logical to discuss interfacial reactions in aqueous biosystems primarily in terms of water wettability, hydrophilicity and water surface tension. Based on these experimentally accessible primary data, derived secondary data on surface energy parameters (e.g. total SFE and polar/dispersive components of SFE) might be calculated and carefully be interpreted.

4. Roughness induced wetting: Theoretical aspects and practical applications

4.1. Wetting phenomena on titanium implant surfaces

Young's equation has been the focus of controversial discussion because of its theoretical derivation and the fact that it is almost impossible to prove experimentally [44]. Real surfaces are characterized in almost all cases by a certain degree of roughness and/or by chemical heterogeneity, thus inducing deviations from an ideal surface. These deviations cause changes in the wetting behavior of a rough and heterogeneous surface compared to a smooth and homogeneous one. Static CAs on smooth titanium have shown great variations, dependent on the history of cleaning and storage. Water CAs on air stored samples have been ~70° to 90°, with much lower CAs found directly after plasma treatments, for example. However, after roughening titanium (e.g. by blasting and/or etching treatments), CAs may increase to as high as 150°, exhibiting almost superhydrophobicity [32,33,78]. Another wetting phenomenon that can be observed on titanium implant surfaces in the course of dynamic CA measurements is CA hysteresis. CA hysteresis indicates, in general, the absence of ideal surface conditions and may be caused by one or more of the following issues: surface deformation; swelling; molecular adsorption from the liquid phase and reorientation of surface groups; or by chemical heterogeneity and roughness, which is mainly the case for solid polymeric, ceramic or metallic biomaterial surfaces [57,79,80].

Author's personal copy

Real surfaces show significant differences in the way an advancing water front wets the surface and the way receding water dewets the pre-wetted surface. The corresponding advancing and receding CAs (θ_{adv}, θ_{rec}) observed during measurements of an implant surface may differ by only few degrees up to several tens of degrees in cases with considerable CA hysteresis $\Delta\theta$:

$$\Delta\theta = \theta_{adv} - \theta_{rec} \geqslant 0 \quad (13)$$

Fig. 5a–f shows force curves detected by tensiometric Wilhelmy experiments during immersion and emersion loops in water for differently modified smooth and rough rectangular titanium discs. The force curves reflect a range of typical wetting phenomena that can be observed. Hysteresis between advancing and receding might be constant during multi-loop Wilhelmy runs, thus indicating thermodynamic CA hysteresis, as typically observed on smooth commercially pure (cp) titanium surfaces (Fig. 5a). The receding CAs, depending on the surface history, may range on smooth titanium from 0° up to ~50°, while the advancing CAs often are near 90° or smaller. This distinct hysteresis can be reduced, for example, by the adsorption of macromolecules onto the surface, as depicted in Fig. 5b. Here, adsorption of albumin led to a stepwise shift of the advancing force loop towards increased hydrophilicity.

The latter is just an example of how the Wilhelmy plate method has generally allowed the investigation of dynamic changes of CAs during biomaterial surface/protein interactions [56,81–83]. At polymeric surfaces, it was observed that both advancing and receding CAs underlie changes during protein adsorption [56,84]. An increase in hysteresis due to shifts of the receding CA only was observed with very low protein concentrations on fluoropolymers, indicating a concentration-dependent sensitivity of advancing and receding CAs [56,85]. Thus, an increase in hysteresis can be attributed to the surface heterogeneity of a patchy overlayer of adsorbed protein [84], whereas a decrease in hysteresis is caused by surface homogenization due to further protein adsorption.

In recent years, in the field of biomaterial/protein interactions, dynamic CA analysis has been combined with different analytical

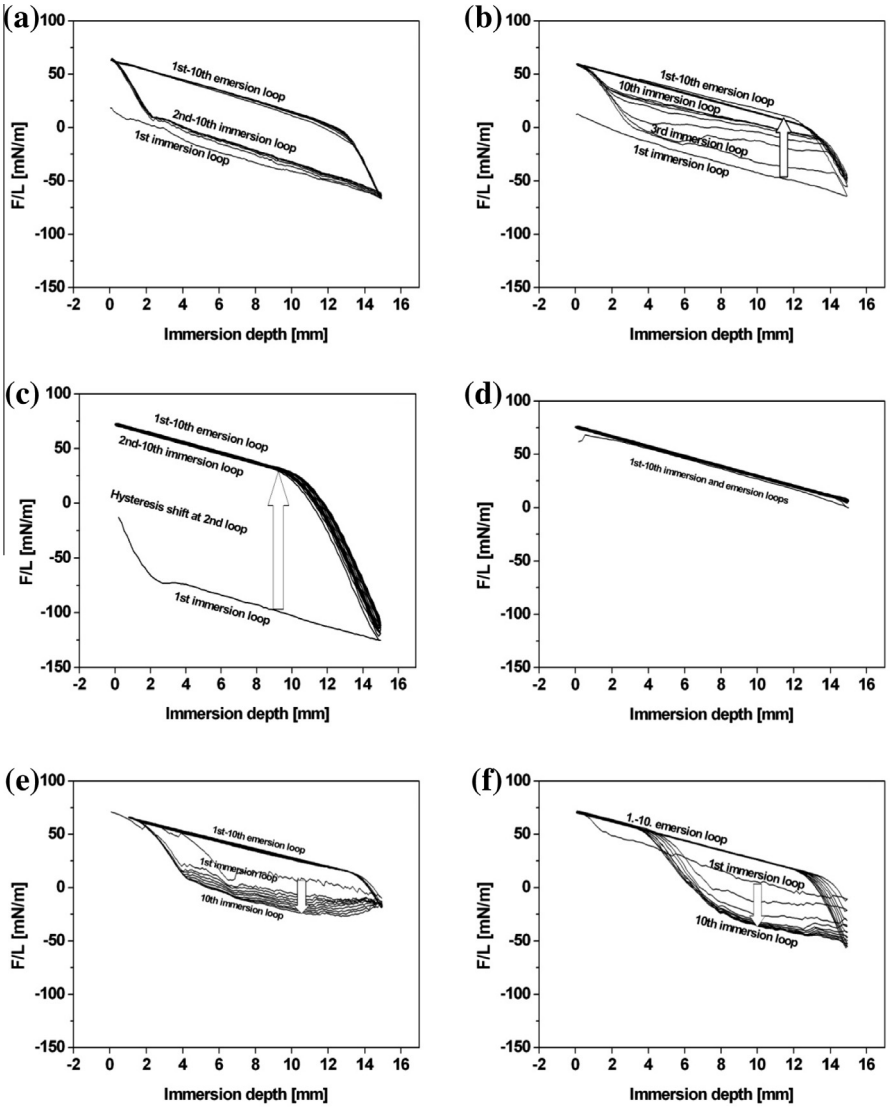

Fig. 5. Wetting phenomena on smooth and rough titanium surfaces based on thermodynamic and kinetic hysteresis observations during tensiometric multi-loop Wilhelmy runs. (a) Thermodynamic hysteresis of a typical cp titanium surface that was ultrasonically cleaned. (b) Protein (i.e. albumin) adsorption on smooth titanium leading to hydrophilization and minimized hysteresis. (c) Initial hydrophobic wetting behavior and thermodynamic hysteresis of microrough titanium surfaces during initial wetting (first loop) and typical shift of microstructured titanium surfaces to hydrophilization during following immersion loops. (d) Constant superhydrophilic wetting behavior of microrough titanium that was either chemically modified [32,62] or modified by nanoscale polycrystalline anatase thin films and irradiated by short-term UV-A [90]. (e, f) Initial hydrophilic wetting behavior and time-dependent step-wise shift to hydrophobicity during following immersion loops of (e) air-based RFGD plasma-treated titanium and of (f) acid-etched titanium (Kroll etchant containing HF and HNO_3). After the tenth loop both surfaces resemble the hysteresis of untreated cp titanium.

Author's personal copy

methods such as reflectometry [86], quartz crystal microbalance [2,87], scanning force spectroscopy [88] or different methods of immunological or biochemical assays for protein quantification [2,78]. Many studies have confirmed that concentration-dependent CAs provide a unique measure of solid–liquid adsorption that has potential in biomaterials research applications involving proteins, as proposed two decades ago [89].

Strong advancing shifts could also be observed on microstructured sandblasted and acid-etched titanium surfaces (Fig. 5c). Whereas the first force loop reflects a very pronounced hysteresis between wetting and de-wetting, confirmed here by the calculated corresponding advancing and receding CAs of 140° and 0°, a sudden shift from hydrophobic to hydrophilic occurred between the initial and all following immersion loops. Indeed, sandblasted and acid-etched surfaces, together with other microstructured titanium implant surfaces, are characterized by such kinetic hysteresis [32]. In contrast, microstructured sandblasted and acid-etched surfaces with increased hydrophilicity exhibit no apparent hysteresis [32,62] (Fig. 5d). Such superhydrophilic wetting has been observed on such hydrophilized specimens and on UV-A activated additive anatase surface modifications of titanium [90].

In the examples presented until now, kinetic hysteresis was caused by an advancing shift towards increased wetting tension. But also the opposite is possible if titanium is freshly prepared by etching procedures. As shown in Fig. 5e and f, plasma-treated or acid-etched titanium samples are initially extremely hydrophilic, showing very small hysteresis for short periods of time. However, these surfaces undergo a very fast hydrophobization of the advancing CA during tensiometry, accompanied by a corresponding increase in hysteresis that finally resembles the wetting state observed with untreated cp titanium [91]. Thus, wetting of titanium in general, but especially the advancing CA, is very variable.

4.2. Wettability models on rough surfaces

As outlined above, wetting phenomena such as CA hysteresis or (super)hydrophobicity, both observed on the titanium oxide surface of titanium implants, are closely related to the surface topography. Fundamental theories of roughness-induced wetting were initially described about 70 years ago [92,93] and are still under intense research due to their widespread technical and biomedical importance. The Wenzel theory evaluates cases in which a wetting liquid completely fills a rough surface topography, including all indentations and pores (Fig. 6). The roughness factor (r_W), as suggested by Wenzel, modulates the immeasurable Young CA (θ_{Young}), thus leading to the experimentally accessible apparent Wenzel CA (θ_W):

$$\cos\theta_W = r_W \cos\theta_{Young} \tag{14}$$

The roughness factor has been defined as ratio of the real surface area to the projected surface area and is therefore on rough surfaces always > 1. The roughness factor is difficult to determine, but the hybrid 3-D roughness parameter S_{dr}, also known as the developed surface area ratio [15], may be used to estimate the Young CA by combining Eqs. (14) and (15) [94].

$$r_W = 1 + S_{dr} \tag{15}$$

S_{dr} expresses the ratio of the increment of the interfacial surface area and the projected area. $S_{dr} = 0$ refers to a totally flat surface, while for example $S_{dr} = 0.5$ indicates an additional surface area of 50% contributed by the texture as compared to an ideal plane. Of practical relevance is an important outcome of Wenzel's relation: because of the sign of the cosine, hydrophilic surfaces with CAs below 90° become more hydrophilic by roughening and hydrophobic surfaces become more hydrophobic if the surfaces are roughened. In the research field of superhydrophobic surfaces, it has been known for several years that roughness has to be applied to hydrophobic surfaces to further increase their hydrophobicity. Noteworthy is the fact that by chemical modification alone, without induced roughness (e.g. smooth fluoropolymeric or wax surfaces), CAs scarcely exceed 120°. CAs in the range of ~125° to nearly 180° are mainly induced by roughness. Recently, Marmur suggested that rough surfaces with CAs beyond the chemically induced hydrophilic or hydrophobic CAs of the unroughened surface should be referred to as parahydrophilic or parahydrophobic [38].

A well-known example of superhydrophobicity is exhibited by the "lotus" surfaces, so-named according to the superhydrophobic surface of the leaves of the sacred lotus plant, which causes water drops to easily roll off and serve as a self-cleaning mechanism to remove particulate contamination from the leaves [95]. Since its discovery, this effect has been found on many plant surfaces and is primarily caused by a combination of micro- and submicro structures. The roughness of the lotus surface is generated by papillose epidermal cells and epicuticular wax crystals, which can entrap air beneath the water drops and lead to CAs exceeding 150°. Resting like a fakir on his bed of nails, a water drop on such a rough surface interacts with a heterogeneous surface composed of the solid material and air (Fig. 6). This wetting situation has been described by Cassie and Baxter [92], who recognized the relation between the apparent CA (θ_{CB}) on a heterogeneous surface and the respective area fractions $f1$, $f2$, and so on, of the components with their respective individual Young CAs. If heterogeneity is caused by air, the CA of water on air should be 180° and the Cassie–Baxter equation is as follows:

$$\cos\theta_{CB} = f\cos\theta_{Young} + f - 1 \tag{16}$$

where f is the area fraction of the solid in contact with the liquid, or in other words, the top portion of all surface protrusions that interact with the liquid and not the surface roughness itself [94]. Strictly speaking, Eq. (16) is limited to surface pillars with flat tops.

The Wenzel and Cassie–Baxter wetting regimes are helpful in understanding the wetting states of biomaterial surfaces, most of which have some level of surface roughness, especially when evaluating strongly hydrophobic CAs beyond 120°. In the case of microrough blasted and acid-etched titanium implant surfaces, high CAs are most probably caused by air trapped underneath the water droplets, according to the Cassie–Baxter regime. However, due to innate surface heterogeneities at the micro- and nanoscales of these industrially produced implants, the possibility exists that some regions of the surface present full liquid penetration into the topography and others show partial or no penetration, increasing the complexity of the surface wetting calculations.

As will be shown ahead, insights into the respective wetting regimes are essential for calculations of SFE on rough or heterogeneous surfaces. A general problem of wetting science is concerned with determining which CAs amongst the available static and dynamic CAs are related to the Wenzel or Cassie–Baxter CAs in Eqs. (14) and (16), respectively. Or, in other words, which apparent CA is the one that can be linked with the Young CA in order to quantify SFE parameters?

Advancing and receding CAs generally determine the upper and lower limits of a range of apparent CAs a drop may rest at in a metastable state on a real surface [37]. The Wenzel or Cassie–Baxter CA lies somewhere in between. Certain techniques have been developed to allow a drop to reach a more stable equilibrium CA on a given surface, characterized by minimized Gibbs energy. To overcome Gibbs energy barriers and thus to measure CA of the drop in its most stable equilibrium on a solid, vibrations have been experimentally applied during goniometric as well as tensiometric CA analyses [41,51,52,80,96–98]. In addition, the CA in most stable

Author's personal copy

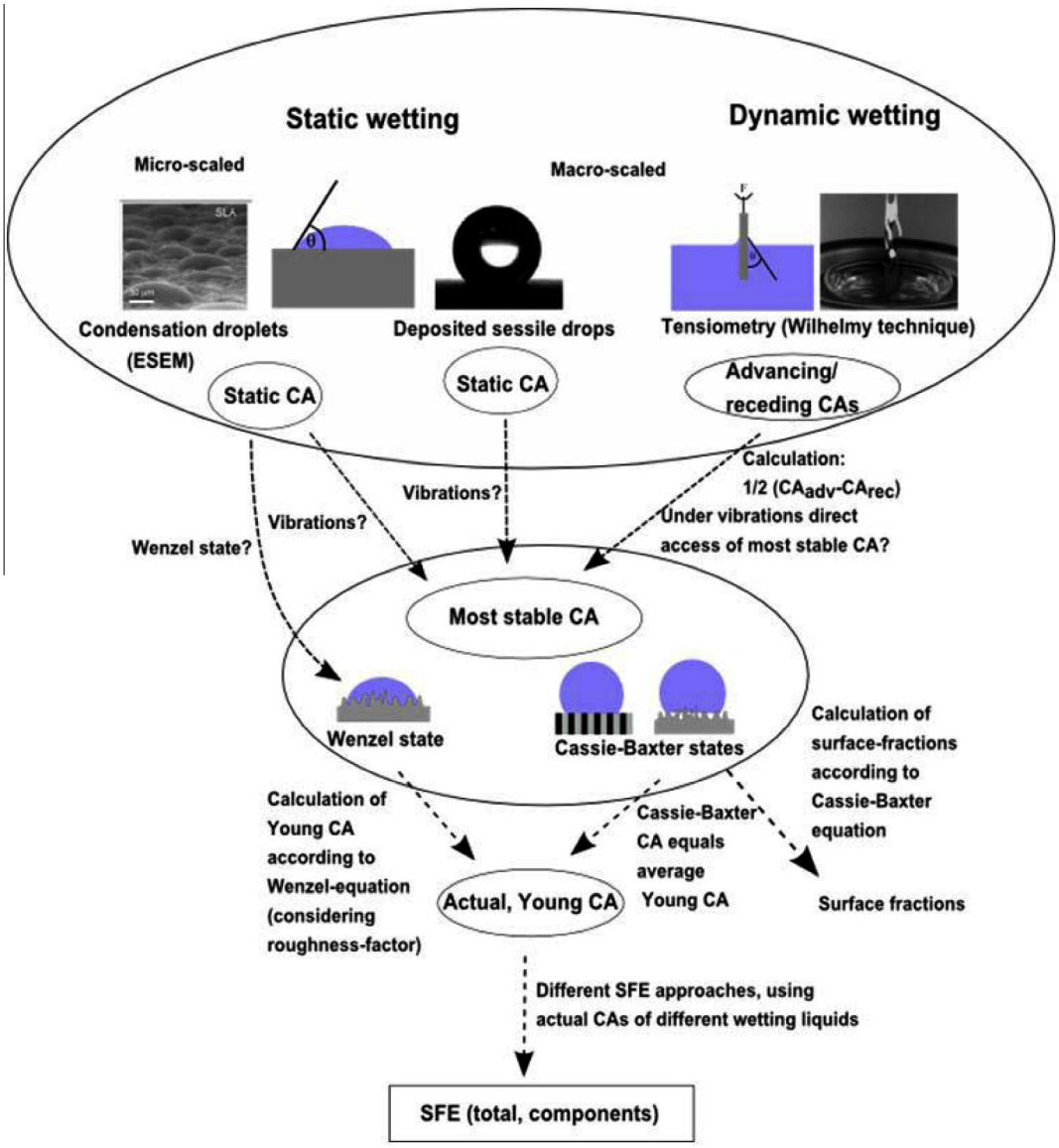

Fig. 6. Wetting analysis on non-ideal rough and/or heterogeneous biomaterial surfaces. Role of the most stable CA for modeling wetting according to the homogeneous or heterogeneous wetting regimes and for the estimation of the Young CA, essential for SFE approaches (based on CA definitions in Ref. [37]).

equilibrium can be roughly estimated based on the average of advancing and receding CAs [50]:

$$\theta_{\text{most stable}} = \frac{(\theta_{\text{adv}} + \theta_{\text{rec}})}{2} \tag{17}$$

However, Eq. (17) is not rooted in any fundamental theory and should be carefully applied [37,51,80].

At this point is clear that the type of CA that is measured during any wetting analysis is of essential importance [37]. From a theoretical point of consideration, the valid calculation of SFE of a solid material based on Young's equation, as described in Eq. (5), can only be performed using CAs of drops that are resting in thermodynamic equilibrium on an ideal solid surface. On rough and heterogeneous surfaces, the Wenzel and Cassie–Baxter equations seem to be good approximations for the most stable CA, associated with the lowest possible Gibbs energy of the wetting system, given that the drop size is sufficiently large compared with the scale of roughness or chemical heterogeneity [37].

To summarize, SFE calculations of rough or heterogeneous surfaces are generally based on the Young equation. However, the required Young CA of a liquid on the respective non-ideal solid cannot be directly measured, but has to be achieved considering the most stable CA, either by averaging the advancing and receding CAs, or by directly measuring this most stable state via applying vibrations to the system [37]. In addition, in the case of rough surfaces the roughness factor has to be considered to finally get the Young CA from the Wenzel equation, which is not a trivial parameter to calculate for the case of randomly patterned surface modifications generally used for implant applications.

Two further models have to be discussed that allow the prediction of superhydrophobic CAs on rough surfaces but without requiring a hydrophobic CA on the original, unroughened material surface. In other words, there are certain surface topographies that are able to make a hydrophilic material hydrophobic, against the Wenzel prediction that roughness should lower the CA in this case. The first are self-affine, mushroom-type or, generally termed, surfaces with multivalued roughness features, where the roughness valleys are interconnected and also connected to the atmosphere [99,100]. Conversely, the second model includes closed-pore, also known as honey-comb surface structures, where single pores are

Author's personal copy

not connected [100,101]. In this case, since the pores are completely enclosed as soon as the wetting liquid rests upon the surface, the liquid will not totally penetrate into the pores because the pressure of entrapped air will increase and thus prevent a complete filling.

At the moment, it is still a puzzling issue to determine which amongst the available models should be applied to a specific complex microstructure [101].Therefore, in the next chapter, we will summarize our current state of knowledge of possible applications of the described models to the observed wetting phenomena on microrough titanium surfaces.

4.3. Application of wetting models to titanium surfaces

A recent study increased our understanding of titanium wetting by performing wettability analyses with several of the techniques described in Section 2, specifically ESEM and classical optical sessile drop on microstructured and micro-/nanostructured implant surfaces [33]. Both types of surfaces, microstructured alone and combined micro-/nanostructured, exhibited more hydrophilic CAs with condensed, nucleated droplets in the submicroscale range as evaluated by ESEM, when compared to deposited sessile drops.

This study, in agreement with earlier experimental results showing strong hydrophobicity evaluated with sessile microdroplets [62,78], suggests that the classical sessile drop method detected a heterogeneous air/material surface (i.e. Cassie–Baxter regime), whereas the smaller, condensed droplets completely filled the material surface structure and avoided any chemical heterogeneity (i.e. Wenzel regime). These results also support studies by other groups, who have observed the evolution of condensed droplets produced on superhydrophobic model surfaces starting with nucleation at the bottom of surface features and resulting in drops finally resting in a Wenzel state, whereas droplets deposited on the same surfaces appeared in a more hydrophobic Cassie–Baxter state [102,103].

Assuming a Wenzel state for the observed nucleated droplets on the microrough titanium specimens, representing an apparent CA of 50° and a roughness factor of 1.7 (unpublished S_{dr} roughness data of 0.7 based on stereo-SEM data), Eq. (14) allows the calculation of the Young CA of the sandblasted and acid-etched surface to be 67°. Thus, the blasted and etched surface appears to have a moderate hydrophilicity when dealing with condensed water droplets. Further studies have to investigate if condensed droplets are equal to the most stable CA or if vibrations have to be applied on such systems. Inserting now the Young CA of the sandblasted and acid-etched surface of 67° into Eq. (16) and using the macroscopically measured, hydrophobic CA of ~140° (under the assumption of a most stable CA), one gets an area fraction f of the solid sandblasted and acid-etched surface in contact with liquid of ~17%. Thus, water faces predominantly air during the first contact with this implant surface in the sessile drop method.

Fig. 6 summarizes the experimentally accessible and theoretically derived CAs in the field of microrough dental implant surfaces and their meaning for SFE calculations. Exemplarily shown here are static CAs of deposited or condensed sessile drops as well as advancing and receding CAs by tensiometry. The most stable CA, characterized by the lowest possible Gibbs energy of the wetting system, can be accessed, as outline above, either by vibrations or by averaging advancing and receding CAs [37]. Finally, applying the Wenzel equation in the case of rough surfaces leads to the Young CA, a prerequisite for SFE calculations.

The above-mentioned lotus surfaces represent, besides others, a special type of superhydrophobic surfaces that have evolved in

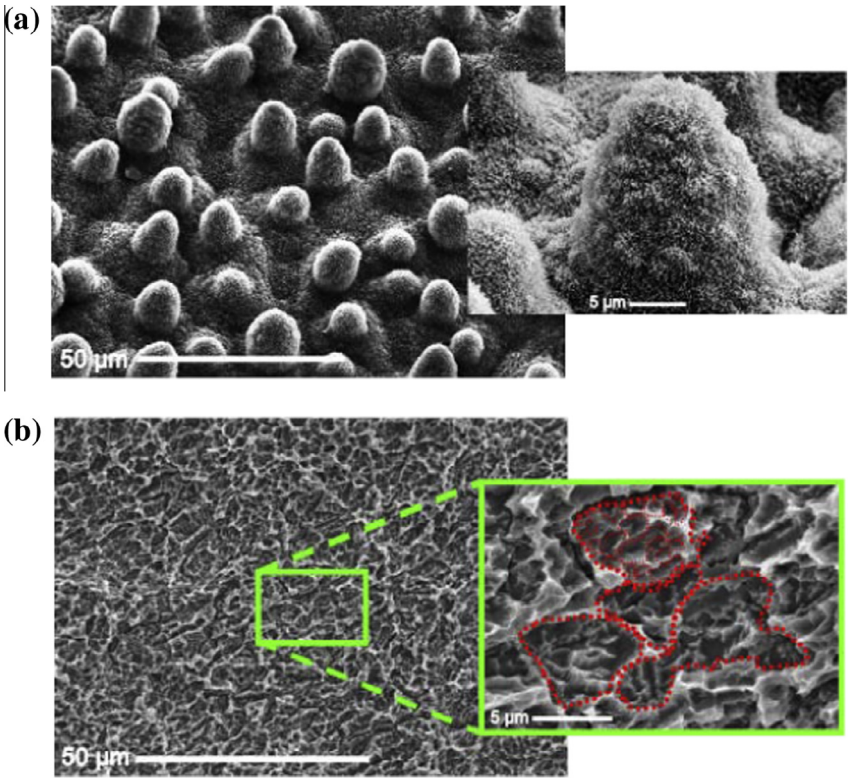

Fig. 7. Examples of hierarchically structured surfaces that lead to hydrophobicity: (a) sacred lotus leaf surface, courtesy of Barthlott and Neinhuis [95] and (b) sandblasted and acid-etched titanium surface. Such composite or hierarchical surface structures, formed on many plants by a combination of two (or more) layers with structures at different scales, is built by convex cells (in the range of 10–50 µm), and a much smaller superimposed layer of hydrophobic 3-D wax tubules (at the scale of 100 nm) [79,106]. In the case of the sandblasted and acid-etched implant, the surface has concave grooves generated by sandblasting (in the range of 5–~70 µm), and by wet acid etching that creates pores of different shapes (in the range of several hundred nanometers up to 3 µm).

Author's personal copy

nature. Strongly hydrophobic, microrough implant surfaces show a certain analogy to lotus surfaces, also being hierarchically structured in the case of combined blasted and acid-etched surfaces (Fig. 7). This hierarchy in their microstructure might, at least partially, force a Cassie–Baxter wetting regime and explain the quite different wetting behavior compared to smooth titanium surfaces. However, the Cassie–Baxter regime, as is the case for lotus surfaces, is typically characterized by a very small CA hysteresis [102].This is not the case for microrough titanium surfaces, as we saw before (Fig. 5c).

The observation that water drops do not always roll off from blasted and etched titanium surfaces when they are tilted indicates high adhesive forces and rather resembles the so-called petal effect [104]. Petal effects have been observed on plant surfaces with hierarchical micro- and nanostructures, being both larger than those found on the lotus leaf, thus inducing a high CA hysteresis. Feng et al. explained this wetting behavior using the Cassie impregnating wetting regime, where water droplets are expected to enter into the larger scale grooves of the petal but not into the smaller ones, leading to a wetting state where larger grooves are wetted but plateaus that are superimposed with smaller grooves are dry [104]. According to this model it is possible that the larger blasted grooves on the titanium surface can initially be filled with water, at least partly, while the smaller etched pores cannot, thus explaining that the surface is strongly hydrophobic with simultaneous strong adhesive forces.

Fig. 7 also illustrates that blasted and etched titanium resembles a closed-pore surface structure due to the chemically etched pores. Therefore, the trapped air, fully isolated from the outer atmosphere, might force the Cassie–Baxter situation. The effect is similar to the petal effect in that the surface is not fully in liquid contact but air is trapped inside the closed pores, thus forcing high CAs. It can be assumed that during the first receding loops of dynamic measurements a thin layer of liquid does stay in the outer part of the pores, thus inducing the very low receding angle and the fully wettable state from the second advancing loop onward. In contrast, in the case of hydrophilized, sandblasted and acid-etched surfaces that have been chemically modified, superhydrophilicity indicates a spontaneous and complete filling of all surface pores.

From the above discussion, it follows that currently the observed wetting phenomena on titanium implant surfaces cannot be fully based solely on the Cassie–Baxter and/or Wenzel regime. If a transition from a Cassie–Baxter to a Wenzel state, as reported by Lafuma and Quéré or by Ishino et al. [102,105], can be assumed for the complex structured blasted and etched titanium surfaces, is still unclear.

Even though the different available wetting models increase our understanding of wetting phenomena, we are far away from predicting the wetting state of a complex structured biomaterial surface. Therefore, considering the available theoretical and applied knowledge of roughness induced wetting seems imperative to avoid producing biomaterial surface topographies with undesired wetting behavior. Due to the capability of micro- and nanoscale surface modifications to affect wetting, be it due to direct alterations to the surface energy or from increased surface area for carbon adsorption, these surfaces should be further analyzed and monitored in emergent new technologies.

In clinical applications, the initial surface wetting of a blasted and acid-etched dental implant with blood can be assumed to follow the Cassie–Baxter regime. Consequently, at least during the initial physiological interactions between blood and the implant, it is possible that only a very small portion of surface area, the top of the protrusions on the surface, are interacting with blood and the rest is predominantly entrapping air.

5. Conclusions

Considering the different types of theoretically based and experimentally accessible CAs, the different approaches to get the most reliable and stable CAs, and being aware of the ongoing discussion about the applicability of the different mathematical approaches for the calculation of SFE based on Young's equation, it seems that our understanding of wetting of real implant surfaces is still in its infancy. Therefore, the control and modulation of the wetting behavior as important requirements that have to be fulfilled in order to render a biomaterial with good biological performance are interdisciplinary challenges. According to the reviewed state of knowledge, the following summary and questions of interest can be outlined.

(1) Hydrophilic surfaces can facilitate the initial interactions between the surface and the wetting liquid, which is relevant for wound healing and osseointegration. However, is superhydrophilicity necessary, or is there a CA range of interest for the best biological performance?
(2) Surface roughness has a significant effect on the wetting behavior, as well as a significant role in the process of osseointegration. Yet, will the required range of CAs to improve biological performance be attainable on the new generation of micro-/nanorough surfaces?
(3) New experimental approaches that use smaller (nano) droplets and provide more stable CAs will enhance our understanding of the wetting of implant surfaces at microscopic scales. Still, can the influence of the different wetting regimes be identified and even quantified in real-life complex surfaces?
(4) Wetting behavior including surface contaminations of implants needs to be critically evaluated to try to determine implant outcomes. Can these parameters be truly controlled up to the time-point of its surgical insertion?
(5) The reviewed principles for the wetting behavior of dental implants are relevant for oral, maxillofacial and orthopedic implant surfaces to produce implants that can promote bone effectively, even in compromised patients.

Acknowledgements

Support of the ITI Foundation (Basel, Switzerland), of the German Research Foundation (DFG, Deutsche Forschungsgemeinschaft, Bonn, Germany) and the Baden-Wuerttemberg Stiftung (Stuttgart, Germany) is gratefully acknowledged.

R.A.G. is thankful for the support of the Government of Panama (IFARHU-SENACYT) and the IMI Program of the National Science Foundation (ICMR Program, Award No. DMR04-09848). B.D.B., Z.S. and R.A.G. are supported by the National Institutes of Health, United States (US PHS Grant AR052102).

Appendix A. Figures with essential color discrimination

Certain figures in this article, particularly Figs. 1, 2, 4, 6 and 7, are difficult to interpret in black and white. The full color images can be found in the on-line version, at http://dx.doi.org/10.1016/j.actbio.2014.02.040.

References

[1] Zhao G, Raines AL, Wieland M, Schwartz Z, Boyan BD. Requirement for both micron- and submicron scale structure for synergistic responses of osteoblasts to substrate surface energy and topography. Biomaterials 2007;28(18):2821–9.
[2] Eichler M, Katzur V, Scheideler L, Haupt M, Geis-Gerstorfer J, Schmalz G, et al. The impact of dendrimer-grafted modifications to model silicon surfaces on

Author's personal copy

protein adsorption and bacterial adhesion. Biomaterials 2011;32(35):9168–79.
[3] Park JH, Wasilewski CE, Almodovar N, Olivares-Navarrete R, Boyan BD, Tannenbaum R, et al. The responses to surface wettability gradients induced by chitosan nanofilms on microtextured titanium mediated by specific integrin receptors. Biomaterials 2012;33(30):7386–93.
[4] Park JH, Olivares-Navarrete R, Wasilewski CE, Boyan BD, Tannenbaum R, Schwartz Z. Use of polyelectrolyte thin films to modulate Osteoblast response to microstructured titanium surfaces. Biomaterials 2012;33(21):5267–77.
[5] Vogler EA. Protein adsorption in three dimensions. Biomaterials 2012;33(5):1201–37.
[6] Kohavi D, Badihi HL, Rosen G, Steinberg D, Sela MN. Wettability versus electrostatic forces in fibronectin and albumin adsorption to titanium surfaces. Clin Oral Implants Res 2013;24(9):1002–8.
[7] Scheideler L, Rupp F, Wendel HP, Sathe S, Geis-Gerstorfer J. Photocoupling of fibronectin to titanium surfaces influences keratinocyte adhesion, pellicle formation and thrombogenicity. Dent Mater 2007;23(4):469–78.
[8] Marshall SJ, Bayne SC, Baier R, Tomsia AP, Marshall GW. A review of adhesion science. Dent Mater 2010;26(2):E11–6.
[9] Duske K, Koban I, Kindel E, Schroder K, Nebe B, Holtfreter B, et al. Atmospheric plasma enhances wettability and cell spreading on dental implant metals. J Clin Periodontol 2012;39(4):400–7.
[10] Schwarz F, Wieland M, Schwartz Z, Zhao G, Rupp F, Geis-Gerstorfer J, et al. Potential of chemically modified hydrophilic surface characteristics to support tissue integration of titanium dental implants. J Biomed Mater Res B 2009;88B(2):544–57.
[11] Adell R, Lekholm U, Rockler B, Branemark PI. A 15-year study of osseointegrated implants in the treatment of the edentulous jaw. Int J Oral Surg 1981;10(6):387–416.
[12] Branemark PI, Adell R, Breine U, Hansson BO, Lindstrom J, Ohlsson A. Intra-osseous anchorage of dental prostheses. I. Experimental studies. Scand J Plast Reconstr Surg 1969;3(2):81–100.
[13] Branemark PI, Hansson BO, Adell R, Breine U, Lindstrom J, Hallen O, et al. Osseointegrated implants in the treatment of the edentulous jaw. Experience from a 10-year period. Scand J Plast Reconstr Surg Suppl 1977;16:1–132.
[14] Albrektsson T, Branemark PI, Hansson HA, Lindstrom J. Osseointegrated titanium implants. Requirements for ensuring a long-lasting, direct bone-to-implant anchorage in man. Acta Orthop Scand 1981;52(2):155–70.
[15] L. Blunt, W.P. Dong, E. Mainsah, N. Luo, T.Mathia, K.J. Stout, et al., Parameters for char acterising 3-D surfaces. In: K.J.Stout (Ed.), Development of methods for the characterization of roughness in three dimensions, Penton Press, London, pp. 230–231.
[16] Wennerberg A, Albrektsson T. Suggested guidelines for the topographic evaluation of implant surfaces. Int J Oral Maxillofac Implants 2000;15(3):331–44.
[17] Wennerberg A, Albrektsson T. Effects of titanium surface topography on bone integration: a systematic review. Clin Oral Implants Res 2009;20:172–84.
[18] Buser D, Janner SF, Wittneben JG, Bragger U, Ramseier CA, Salvi GE. 10-year survival and success rates of 511 titanium implants with a sandblasted and acid-etched surface: a retrospective study in 303 partially edentulous patients. Clin Implant Dent Relat Res 2012;14(6):839–51.
[19] Chappuis V, Buser R, Bragger U, Bornstein MM, Salvi GE, Buser D. Long-term outcomes of dental implants with a titanium plasma-sprayed surface: a 20-year prospective case series study in partially edentulous patients. Clin Implant Dent Relat Res 2013;15(6):780–90.
[20] Cochran DL, Jackson JM, Jones AA, Jones JD, Kaiser DA, Taylor TD, et al. A 5-year prospective multicenter clinical trial of non-submerged dental implants with a titanium plasma-sprayed surface in 200 patients. J Periodontol 2011;82(7):990–9.
[21] Levine RA, Sendi P, Bornstein MM. Immediate restoration of nonsubmerged titanium implants with a sandblasted and acid-etched surface: five-year results of a prospective case series study using clinical and radiographic data. Int J Periodontics Restorative Dent 2012;32(1):39–47.
[22] Gittens RA, Olivares-Navarrete R, McLachlan T, Cai Y, Hyzy SL, Schneider JM, et al. Differential responses of osteoblast lineage cells to nanotopographically-modified, microroughened titanium-aluminum-vanadium alloy surfaces. Biomaterials 2012;33(35):8986–94.
[23] Hayashi M, Jimbo R, Lindh L, Sotres J, Sawase T, Mustafa K, et al. In vitro characterization and osteoblast responses to nanostructured photocatalytic TiO_2 coated surfaces. Acta Biomater 2012;8(6):2411–6.
[24] Wennerberg A, Svanborg LM, Berner S, Andersson M. Spontaneously formed nanostructures on titanium surfaces. Clin Oral Implants Res 2013;24(2):203–9.
[25] Baier RE, Meyer AE, Natiella JR, Natiella RR, Carter JM. Surface properties determine bioadhesive outcomes: methods and results. J Biomed Mater Res 1984;18(4):337–55.
[26] Baier RE, Meyer AE. Future directions in surface preparation of dental implants. J Dent Educ 1988;52(12):788–91.
[27] Kasemo B, Lausmaa J. Biomaterial and implant surfaces: on the role of cleanliness, contamination, and preparation procedures. J Biomed Mater Res 1988;22(A2 Suppl.):145–58.
[28] Kilpadi DV, Lemons JE. Surface energy characterization of unalloyed titanium implants. J Biomed Mater Res 1994;28(12):1419–25.
[29] Schwartz Z, Boyan BD. Underlying mechanisms at the bone–biomaterial interface. J Cell Biochem 1994;56(3):340–7.
[30] Kieswetter K, Schwartz Z, Dean DD, Boyan BD. The role of implant surface characteristics in the healing of bone. Crit Rev Oral Biol Med 1996;7(4):329–45.
[31] Steinberg D, Klinger A, Kohavi D, Sela MN. Adsorption of human salivary proteins to titanium powder. I. Adsorption of human salivary albumin. Biomaterials 1995;16(17):1339–43.
[32] Rupp F, Scheideler L, Eichler M, Geis-Gerstorfer J. Wetting behavior of dental implants. Int J Oral Maxillofac Impl 2011;26(6):1256–66.
[33] Gittens RA, Olivares-Navarrete R, Cheng A, Anderson DM, McLachlan T, Stephan I, et al. The roles of titanium surface micro/nanotopography and wettability on the differential response of human osteoblast lineage cells. Acta Biomater 2013;9:6268–77.
[34] Buser D, Broggini N, Wieland M, Schenk RK, Denzer AJ, Cochran DL, et al. Enhanced bone apposition to a chemically modified SLA titanium surface. J Dent Res 2004;83(7):529–33.
[35] Khandelwal N, Oates TW, Vargas A, Alexander PP, Schoolfield JD, Alex MC. Conventional SLA and chemically modified SLA implants in patients with poorly controlled type 2 diabetes mellitus – a randomized controlled trial. Clin Oral Implants Res 2013;24(1):13–9.
[36] Schindelholz E, Kelly RG. Wetting phenomena and time of wetness in atmospheric corrosion: a review. Corros Rev 2012;5–6:135–207.
[37] Marmur A. A guide to the equilibrium contact angles maze. In: Mittal KL, editor. Contact angle, wettability and adhesion. Leiden: Koninklijke Brill NV; 2009. p. 3–18.
[38] Marmur A. Hydro- hygro- oleo- omni-phobic? Terminology of wettability classification. Soft Matter 2012;8(26):6867–70.
[39] Brandon S, Haimovich N, Yeger E, Marmur A. Partial wetting of chemically patterned surfaces: the effect of drop size. J Colloid Interface Sci 2003;263(1):237–43.
[40] Marmur A. Solid-surface characterization by wetting. Ann Rev Mater Res 2009;39:473–89.
[41] Meiron TS, Marmur A, Saguy IS. Contact angle measurement on rough surfaces. J Colloid Interface Sci 2004;274(2):637–44.
[42] Wolansky G, Marmur A. Apparent contact angles on rough surfaces: the Wenzel equation revisited. Colloid Surf A 1999;156(1–3):381–8.
[43] Checco A, Guenoun P, Daillant J. Nonlinear dependence of the contact angle of nanodroplets on contact line curvature. Phys Rev Lett 2003;91(18).
[44] Mendez-Vilas A, Jodar-Reyes AB, Gonzalez-Martin ML. Ultrasmall liquid droplets on solid surfaces: production, imaging, and relevance for current wetting research. Small 2009;5(12):1366–90.
[45] Donald AM. The use of environmental scanning electron microscopy for imaging wet and insulating materials. Nat Mater 2003;2(8):511–6.
[46] Rykaczewski K, Scott JHJ, Fedorov AG. Electron beam heating effects during environmental scanning electron microscopy imaging of water condensation on superhydrophobic surfaces. Appl Phys Lett 2011;98(9).
[47] Marmur A. Line tension and the intrinsic contact angle in solid–liquid–fluid systems. J Colloid Interface Sci 1997;186(2):462–6.
[48] Marmur A, Krasovitski B. Line tension on curved surfaces: liquid drops on solid micro- and nanospheres. Langmuir 2002;18(23):8919–23.
[49] Stockelhuber KW, Radoev B, Schulze HJ. Some new observations on line tension of microscopic droplets. Colloid Surf A 1999;156(1–3):323–33.
[50] Andrieu C, Sykes C, Brochard F. Average spreading parameter on heterogeneous surfaces. Langmuir 1994;10(7):2077–80.
[51] Cwikel D, Zhao Q, Liu C, Su XJ, Marmur A. Comparing contact angle measurements and surface tension assessments of solid surfaces. Langmuir 2010;26(19):15289–94.
[52] Decker EL, Garoff S. Using vibrational noise to probe energy barriers producing contact angle hysteresis. Langmuir 1996;12(8):2100–10.
[53] Andrade JD, Smith LM, Gregonis DE. The contact angle and interface energetic. In: Andrade JD, editor. Surface and interfacial aspects of biomedical polymers. New York: Plenum Press; 1985. p. 249–92.
[54] Lander LM, Siewierski LM, Brittain WJ, Vogler EA. A systematic comparison of contact-angle methods. Langmuir 1993;9(8):2237–9.
[55] Wang JH, Claesson PM, Parker JL, Yasuda H. Dynamic contact angles and contact-angle hysteresis of plasma polymers. Langmuir 1994;10(10):3887–97.
[56] Rupp F, Axmann D, Ziegler C, Geis-Gerstorfer J. Adsorption/desorption phenomena on pure and Teflon((R)) AF-coated titania surfaces studied by dynamic contact angle analysis. J Biomed Mater Res 2002;62(4):567–78.
[57] Good RJ. Contact angle, wetting and adhesion: a critical review. In: Mittal KL, editor. Contact angle, wettability and adhesion. VSP, Utrecht, 1993, p. 3–36.
[58] Krishnan A, Liu YH, Cha P, Woodward R, Allara D, Vogler EA. An evaluation of methods for contact angle measurement. Colloid Surf B 2005;43(2):95–8.
[59] Menzies KL, Jones L. The impact of contact angle on the biocompatibility of biomaterials. Optom Vis Sci 2010;87(6):387–99.
[60] Ruiz-Cabello FJM, Rodriguez-Valverde MA, Marmur A, Cabrerizo-Vilchez MA. Comparison of sessile drop and captive bubble methods on rough homogeneous surfaces: a numerical study. Langmuir 2011;27(15):9638–43.
[61] Young T. An essay on the cohesion of fluids. Phil Trans Roy Soc (London) 1805;95:65–87.
[62] Rupp F, Scheideler L, Olshanska N, de Wild M, Wieland M, Geis-Gerstorfer J. Enhancing surface free energy and hydrophilicity through chemical modification of microstructured titanium implant surfaces. J Biomed Mater Res A 2006;76A(2):323–34.
[63] Rosina J, Kvasnak E, Suta D, Kolarova H, Malek J, Krajci L. Temperature dependence of blood surface tension. Physiol Res 2007;56:S93–8.

Author's personal copy

[64] Craig RG, Berry GC, Peyton FA. Wetting of poly-(methyl methacrylate) and polystyrene by water and saliva. J Phys Chem 1960;64(5):541–3.
[65] Hilditch CJ, Mcevoy RD, George KE, Thompson CC, Ryan MK, Rischmueller M, et al. Upper airway surface tension but not upper airway collapsibility is elevated in primary Sjogren's syndrome. Sleep 2008;31(3):367–74.
[66] Owens DK, Wendt RC. Estimation of the surface free energy of polymers. J Appl Polym Sci 1969;13(8):1741–7.
[67] Kaelble DH. Dispersion-polar surface tension properties of organic solids. J Adhesion 1970;2(2):66–81.
[68] van Oss CJ, Chaudhury MK, Good RJ. Interfacial Lifshitz–van der Waals and polar interactions in macroscopic systems. Chem Rev 1988;88:927–41.
[69] van Oss CJ. Hydrophobicity of biosurfaces – origin, quantitative determination and interaction energies. Colloid Surf B 1995;5:91–110.
[70] Bellon-Fontaine MN, Mozes N, van der Mei HC, Sjollema J, Cerf O, Rouxhet PG, et al. A comparison of thermodynamic approaches to predict the adhesion of dairy microorganisms to solid substrata. Cell Biophys 1990;17(1):93–106.
[71] Combe EC, Owen BA, Hodges JS. A protocol for determining the surface free energy of dental materials. Dent Mater 2004;20(3):262–8.
[72] Shalel-Levanon S, Marmur A. Validity and accuracy in evaluating surface tension of solids by additive approaches. J Colloid Interface Sci 2003;262(2):489–99.
[73] Marmur A, Valal D. Correlating interfacial tensions with surface tensions: a Gibbsian approach. Langmuir 2010;26(8):5568–75.
[74] Sharma PK, Rao KH. Analysis of different approaches for evaluation of surface energy of microbial cells by contact angle goniometry. Adv Colloid Interface Sci 2002;98(3):341–463.
[75] Harnett EM, Alderman J, Wood T. The surface energy of various biomaterials coated with adhesion molecules used in cell culture. Colloid Surf B 2007;55(1):90–7.
[76] Sardin S, Morrier JJ, Benay G, Barsotti O. In vitro streptococcal adherence on prosthetic and implant materials. Interactions with physicochemical surface properties. J Oral Rehabil 2004;31(2):140–8.
[77] Vogler EA. Structure and reactivity of water at biomaterial surfaces. Adv Colloid Interface Sci 1998;74:69–117.
[78] Rupp F, Scheideler L, Rehbein D, Axmann D, Gels-Gerstorfer J. Roughness induced dynamic changes of wettability of acid etched titanium implant modifications. Biomaterials 2004;25(7–8):1429–38.
[79] Quere D. Wetting and roughness. Ann Rev Mater Res 2008;38:71–99.
[80] Martinelli E, Galli G, Cwikel D, Marmur A. Wettability and surface tension of amphiphilic polymer films: time-dependent measurements of the most stable contact angle. Macromol Chem Phys 2012;213(14):1448–56.
[81] Davies J, Nunnerley CS, Paul AJ. A correlative study of the measurement of protein adsorption to steel, glass, polypropylene, and silicone surfaces using ToF-SIMS and dynamic contact angle analyses. Colloid Surf B 1996;6(3):181–90.
[82] do Serro APVA, Fernandes AC, de Jesus B, Saramago V. The influence of proteins on calcium phosphate deposition over titanium implants studied by dynamic contact angle analysis and XPS. Colloid Surf B 1997;10(2):95–104.
[83] Ueda T, Ishihara K, Nakabayashi N. Adsorption–desorption of proteins on phospholipid polymer surfaces evaluated by dynamic contact-angle measurement. J Biomed Mater Res 1995;29(3):381–7.
[84] Kajiyama T, Takahara A. Surface properties and platelet reactivity of segmented poly(etherurethanes) and poly(etherurethaneureas). J Biomater Appl 1991;6(1):42–71.
[85] Dettre RH, Johnson RE. Contact angle hysteresis. IV. Contact angle measurements on heterogeneous surfaces. J Phys Chem 1964;68:1744–50.
[86] do Serro APVA, Fernandes AC, Saramago BDV, Norde W. Bovine serum albumin adsorption on titania surfaces and its relation to wettability aspects. J Biomed Mater Res 1999;46(3):376–81.
[87] Stadler H, Mondon M, Ziegler C. Protein adsorption on surfaces: dynamic contact-angle (DCA) and quartz-crystal microbalance (QCM) measurements. Anal Bioanal Chem 2003;375(1):53–61.
[88] Muller C, Wald J, Hoth-Hannig W, Umanskaya N, Scholz D, Hannig M, et al. Protein adhesion on dental surfaces – a combined surface analytical approach. Anal Bioanal Chem 2011;400(3):679–89.
[89] Vogler EA. Practical use of concentration-dependent contact angles as a measure of solid liquid adsorption. 2. Experimental aspects. Langmuir 1992;8(8):2013–20.
[90] Rupp F, Haupt M, Klostermann H, Kim HS, Eichler M, Peetsch A, et al. Multifunctional nature of UV-irradiated nanocrystalline anatase thin films for biomedical applications. Acta Biomater 2010;6(12):4566–77.
[91] Rupp F, Scheideler L, Geis-Gerstorfer J. Effect of heterogenic surfaces on contact angle hysteresis: dynamic contact angle analysis in material sciences. Chem Eng Technol 2002;25(9):877–82.
[92] Cassie ABD, Baxter S. Wettability of porous surfaces. Trans Faraday Soc 1944;40:546–51.
[93] Wenzel RN. Resistance of solid surfaces to wetting by water. Ind Eng Chem 1936;28:988–94.
[94] Qu AL, Wen XF, Pi PH, Cheng J, Yang ZR. Morphologies and superhydrophobicity of hybrid film surfaces based on silica and fluoropolymer. J Mater Sci Technol 2008;24(5):693–9.
[95] Barthlott W, Neinhuis C. Purity of the sacred lotus, or escape from contamination in biological surfaces. Planta 1997;202(1):1–8.
[96] Smith T, Lindberg G. Effect of acoustic energy on contact angle measurements. J Colloid Interface Sci 1978;66:363–6.
[97] Volpe CD, Maniglio D, Siboni S, Morra M. An experimental procedure to obtain the equilibrium contact angle from the Wilhelmy method. Oil Gas Sci Technol 2001;56(1):9–22.
[98] Volpe CD, Maniglio D, Morra M, Siboni S. The determination of a 'stable-equilibrium' contact angle on heterogeneous and rough surfaces. Colloid Surf A 2002;206(1–3):47–67.
[99] Herminghaus S. Roughness-induced non-wetting. Europhys Lett 2000;52(2):165–70.
[100] Marmur A. From hygrophilic to superhygrophobic: theoretical conditions for making high-contact-angle surfaces from low-contact-angle materials. Langmuir 2008;24(14):7573–9.
[101] Liu JL, Feng XQ, Wang GF, Yu SW. Mechanisms of superhydrophobicity on hydrophilic substrates. J Phys-Condens Matter 2007;19(35).
[102] Lafuma A, Quere D. Superhydrophobic states. Nat Mater 2003;2(7):457–60.
[103] Narhe RD, Beysens DA. Water condensation on a super-hydrophobic spike surface. Europhys Lett 2006;75(1):98–104.
[104] Feng L, Zhang YA, Xi JM, Zhu Y, Wang N, Xia F, et al. Petal effect: a superhydrophobic state with high adhesive force. Langmuir 2008;24(8):4114–9.
[105] Ishino C, Okumura K, Quere D. Wetting transitions on rough surfaces. Europhys Lett 2004;68(3):419–25.
[106] Yan YY, Gao N, Barthlott W. Mimicking natural superhydrophobic surfaces and grasping the wetting process: a review on recent progress in preparing superhydrophobic surfaces. Adv Colloid Interface Sci 2011;169(2):80–105.